




Interfacial phenomena between molten iron and molten slag—Effect of nitrogen on the Marangoni convection

Taishi Matsushita^{1,*} , Ilja Belov¹, Dimitrios Sifarakas¹, Anders E. W. Jarfors¹, and Masahito Watanabe²

¹School of Engineering, Jönköping University, Jönköping, Sweden

²Department of Physics, Gakushuin University, Tokyo, Japan

Received: 4 September 2020

Accepted: 21 December 2020

Published online:
13 January 2021

© The Author(s) 2021

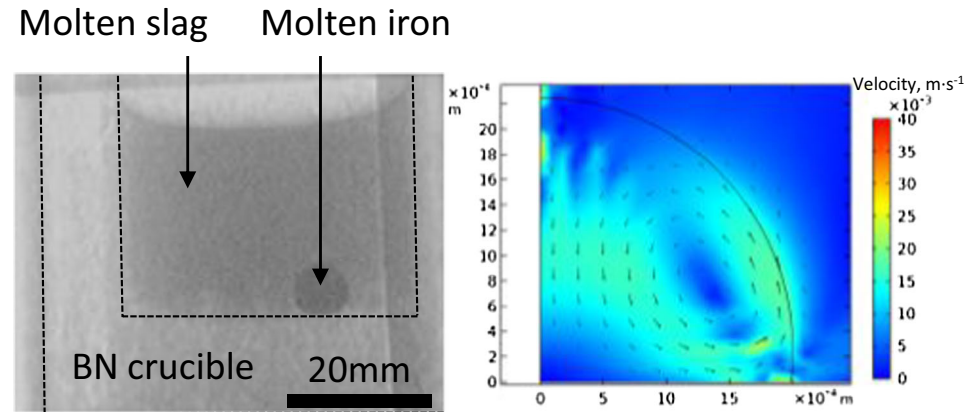
ABSTRACT

In order to investigate the influence of the surface-active element on the interfacial phenomena between molten iron and molten $\text{Al}_2\text{O}_3\text{-CaO-SiO}_2$ slag, a mildly surface-active element, nitrogen, was introduced, and the interfacial phenomena were directly observed using an X-ray sessile drop method. The multiphysics model was employed to calculate the velocity of the Marangoni convection caused by the surface/interfacial tension gradient along with the contour of the sessile drop. Movement of the sessile drop was observed in the experiment, and the driving force of the movement was discussed from the distribution of surface tension active element viewpoint. The calculated velocity of the Marangoni convection in the droplet was reasonably agreed with the literature data for the metal-gas system, and thus, the same model was applied for the metal-slag system. The velocity of the Marangoni convection for the metal-slag system becomes ten times lower compared to that of metal-gas system.

Handling Editor: M. Grant Norton.

Address correspondence to E-mail: taishi.matsushita@ju.se

GRAPHICAL ABSTRACT



Introduction

The Marangoni convection is a flow along with surface/interface caused by the surface tension gradient along with the surface/interface, and such surface-interfacial tension gradient is induced by (1) the temperature gradient, (2) the concentration gradient of surface-active elements and (3) the electrical potential gradient. The Marangoni effect is important not only for the metallurgical process but also in many other fields including medical science and biotechnology [1], and thus, many research works on the Marangoni effect were done since a long time ago. In recent years, extensive studies have done by utilising the microgravity condition to avoid the density convection due to the gravity, to avoid the contamination from the container, to levitate the samples, etc. [2]. Also, the interfacial tension measurements between molten metal and molten slag have been planned [3], and the experiments are currently ongoing on the International Space Station (ISS), Kibo module. The present study is a collaboration between the interfacial tension measurement project by the Japan Aerospace Exploration Agency (JAXA) and the project for the measurement of viscosity of molten slag, and interfacial tension measurement which is funded by Swedish National Space Agency (SNSA).

The Marangoni convection in the elevated temperature system has been studied by many

researchers in the past. For instance, in a molten NaNO_3 column, the Marangoni convection from the higher temperature region, i.e. lower surface tension region, to the lower temperature region, i.e. higher surface tension region was observed [4]. The Marangoni flow due to the concentration gradient was found in the observation of corrosion of refractories by molten metal and molten slag [5]. The Marangoni convection due to the electrical potential change was observed as a spreading and shrinking of a slag droplet on molten metal [6].

In addition to the above-mentioned Marangoni convection, the movement of fine particles such as bubbles and inclusions in molten metal is also explained based on the surface- interfacial tension gradient, and it is treated as a “Marangoni effect” in a broad sense (for details see refs. [1, 7–9]). Such discussion can be utilised to suppress defects in the casting, the nozzle clogging in the continuous casting process, etc. [10].

It is well-known that the Marangoni convection (Marangoni effect) is playing an important role in metallurgical processes. For example, Marangoni convection will enhance the mass transfer, and thus, heterogeneous reaction rate will become higher when the mass transfer process is a rate-controlling step [11]. In such processes, the surface tension of molten metal and slag is relatively high, and also there are surface-active elements (components) for these systems, and thus, the Marangoni convection is induced

relatively easily. The Marangoni convection will also become a cause of interface turbulence since the flow is most intensive at the interface. Such turbulence at the molten mould flux and molten steel interface will lead the entrapment of mould flux into molten steel resulting in the defects. The Marangoni convection and its direction in the weld pool, which is formed in the welding process, have also been investigated by many researchers in the past [12–14]. There are some techniques for the in-situ observation of Marangoni flow, but the observation by a scanning laser microscope is one of the efficient technique for the surface flow observation [15]. The Marangoni convection is often discussed for the single crystal growth of silicon, and the Marangoni convection in the molten silicon was confirmed by a microgravity experiment [16].

Apart from above-mentioned phenomena, the dissolution and adsorption rate of nitrogen gas into molten iron and desorption rate of nitrogen from molten iron were studied by many researchers, and it is concluded that the experimental results can be explained so-called blocking mechanism [17, 18] and change in the surface tension gradient (surface activeness), i.e. Marangoni convection [19, 20].

As described above, there are many examples of the relation between the Marangoni effect and metallurgical processes. In these examples, the Marangoni convection due to the concentration gradient of surface-active elements is one of the interesting phenomena. Adsorption of the surface-active elements and its concentration gradient is closely related to the surface dilatational viscosity and related interfacial phenomena in the metallurgical processes, e.g. foaming, coalescence of bubbles, droplets and solid particles in liquid and also the dispersion of bubbles, droplets as well as solid particles into liquid [21, 22]. The research work on the surface dilatational viscosity for the high-temperature system is scarce; however, there are some works in the field of colloid science [23–26].

Some researches on the effect of surface-active elements on the interfacial phenomena between molten slag and molten metal, including the movement and deformation of the sessile drop have been done [27–31]. In the present study, to understand the role of the surface-active element and its concentration gradient on the Marangoni convection, an experimental set up is designed. Nitrogen is known as a mildly surface-active element [32, 33] although it

is not a strong surface-active element as oxygen, sulphur, selenium and tellurium. Therefore, it can be easily imagined that the Marangoni convection can be induced by the concentration gradient of the nitrogen along with the slag-metal interface. Hence, in the present experiment, the nitrogen as a surface-active element was introduced to the molten iron droplet, which is immersed in the $\text{Al}_2\text{O}_3\text{-CaO-SiO}_2$ molten slag, through the dissolution of boron nitride and the interfacial phenomena (movement and shape of the iron droplet) was observed using X-ray furnace. The results were discussed based on the calculation results of the velocity of Marangoni convection. The velocity of Marangoni convection was calculated by using a commercially available calculation software which allows combining different physical models, so-called multiphysics model.

In the steelmaking process, the nitrogen in the gas phase might reach the molten metal phase through the molten slag phase, and the nitrogen absorption may occur. On the other hand, the feasibility of the denitrification by the molten slag is also considered. In these processes, the mass transfer in the molten metal phase is an important factor, and the Marangoni convection is playing an important role for it. The results of the present study will give some insights to discuss the mass transfer in the molten metal phase, which contact with a molten slag phase.

Experimental

Materials

The $\text{Al}_2\text{O}_3\text{-CaO-SiO}_2$ slag was made from reagents of SiO_2 , (Sigma-Aldrich, – 325 mesh, 99.5% trace metal basis), Al_2O_3 (Sigma-Aldrich, α -phase, –100 mesh, 99%) and CaO. CaO was produced by heating up CaCO_3 powder (Sigma-Aldrich, ACS reagent, $\geq 99\%$) to 1223 K for 12 h in a muffle furnace. The powders were mixed using a mortar and a muller to obtain the desired slag composition (36mass% Al_2O_3 , 50 mass% CaO and 14 mass% SiO_2). As a metal, cylindrical iron rod (5 mm in diameter and 8 mm in length (Alfa Aesar, 99.995%) was used. The dimension of BN crucible (Tanso AB, Sweden, $> 99\%$) is 45 mm in inner diameter and 90 mm in inner height.

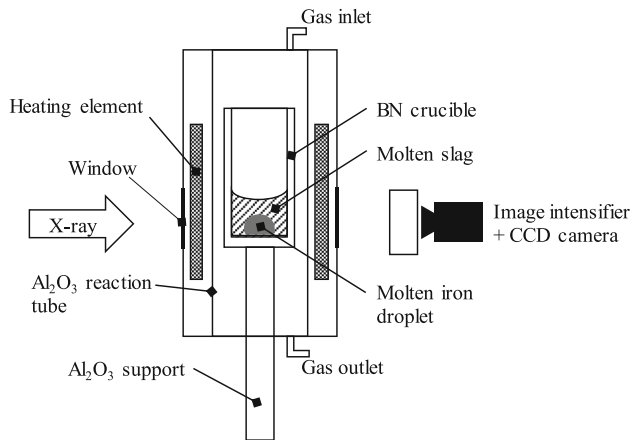


Figure 1 A schematic illustration of the experimental setup.

Apparatus

The apparatus used for the sessile drop measurements consisted of an X-ray unit equipped with an image analyser and a resistance furnace. A schematic diagram of the experimental apparatus is shown in Fig. 1.

The X-ray unit and the high-temperature furnace was employed to observe the metal drop immersed in the slag in order to monitor the interfacial phenomena and the shape of the sessile drop. The X-ray unit used was a Philips BV Pulsera imaging system (Philips, Amsterdam, The Netherlands) with an X-ray source of max. 120 kV. The imaging system consists of a CCD camera with digital noise reduction. The recording system consists of a PC equipped with an image acquisition card which allows to record the X-ray images with 25 fps. The furnace used in the experiments was acquired from Entech Energiteknik AB, Sweden. It is equipped with MoSi_2 heating elements. The furnace temperature was controlled by a type B thermocouple. The windows of 70 mm in the square were provided on both sides of the furnace, which allows the X-ray path through from the source to the detector. A recrystallised Al_2O_3 reaction tube, with an inner diameter of 60 mm, was positioned vertically in the furnace.

Procedure

The iron specimen was placed at the bottom of a boron nitride crucible and immersed in the slag. The boron nitride crucible was placed at the even temperature zone in the reaction tube. Extreme care was taken so that the bottom of the crucible becomes

horizontal. After the attainment of the experimental temperature, namely, 1873 K, the shape and movement of the iron droplet were observed with the aid of the X-ray radiographic apparatus. The experiments were carried out under Ar atmosphere.

Results and discussion

X-ray observation

Some typical X-ray images of the molten iron droplet, which is immersed in the molten slag are shown in Fig. 2. During the observation, it was observed that the sessile drop moved from side to side, and occasionally, the movement was stagnated. The movement of the droplet became moderate with time. The movement of the droplet was observed for approximately 30 min. (including the time from melting point to reach at 1873 K). The maximum moving velocity which was observed in the experiment was approximately $0.005 \text{ m} \cdot \text{s}^{-1}$, i.e. the iron droplet was moved 4.4 mm in 0.88 s. as shown in Fig. 2 (Note that the frame rate of the video recording is 25 fps, and thus, the error in time is $\pm 0.02 \text{ s}$). The nitrogen concentration in the metal drop was analysed after the experiment, and it was found as 0.007 mass%.

According to thermodynamic data [34], ΔG° of the reaction $\text{BN(s)} = \underline{\text{B}} + \underline{\text{N}}$ is

$$\Delta G^\circ = 192000 - 88.7T \text{ J/mol} - \text{BN} \quad (1)$$

Hence, at 1873 K, the boron and nitrogen will dissolve into molten iron so that it satisfies $a_{\underline{\text{B}}}a_{\underline{\text{N}}} = 0.190$, where a is the activity, and the underbar denotes dissolved element.

Regarding the dissolution rate of BN into molten iron, according to Iyengar and Pehlke [35], dissolution rate at 1873 K for unalloyed iron melt is constant up to approximately 30 min, and after that, it becomes moderate. This duration corresponds to the time when the movement of the droplet became moderate (the time required to increase temperature from the melting point of iron (1811 K) to the experimental temperature (approximately 6 min) is ignored). From this fact, the movement of the sessile drop is influenced by the behaviour of the nitrogen as a surface-active element; in other words, the interfacial tension change. More precisely, the driving forces of the movement of sessile drop are:

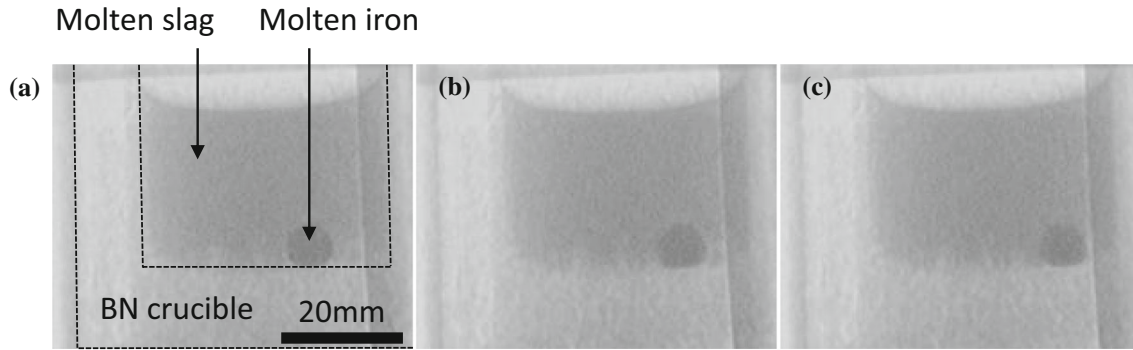


Figure 2 X-ray images of the movement of the molten iron droplet in the molten slag. **a** 0 s, **b** 0.44 s and **c** 0.88 s.

- (1) Force (interfacial tension) difference between one side and another side (e.g. left and right) of the droplet due to the difference of nitrogen distribution and contact angle.
- (2) Marangoni convection in the droplet, which is induced by the nitrogen concentration gradient (interfacial tension gradient) between the bottom part and top part of the droplet.

In the present study, the nitrogen is supplied from the bottom part of the droplet. However, in practice, the nitrogen distribution is not symmetric, and there is nitrogen distribution difference (Hereafter, the nitrogen amount on the left and right sides of the droplet is discussed for the simplicity). For example, it is known that the interfacial tension between molten iron and molten slag decreases with increasing of surface-active element content [36]. Therefore, as shown in Fig. 3, if the nitrogen concentration on the left side is higher than that of the right side, the interfacial tension on the left side (σ_L) becomes lower than that of the right side σ_R , and the net horizontal force will be decided by these interfacial tensions and the contact angle of each side (θ_L and θ_R) as described in Young’s equation. This horizontal force can be the driving force of the movement of the droplet.

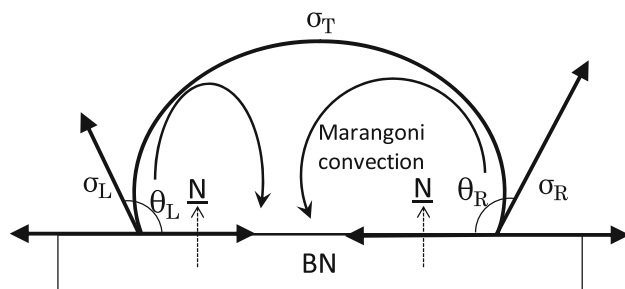


Figure 3 A schematic illustration of the droplet.

Once the droplet starts to move, the droplet will be subjected to the resistance from the molten slag. As mentioned above, the maximum moving velocity of the droplet was $0.005 \text{ m} \cdot \text{s}^{-1}$. The velocity is relatively low, and the size of the object is relatively small. It implies that the droplet will be subjected to the viscous resistance. If it is assumed that the shape of the droplet is a spherical shaped rigid body, the viscous resistance

$$F = 6\pi\eta rv = 5.74 \times 10^{-5} \text{N} \tag{2}$$

where η is the viscosity of slag ($203 \times 10^{-3} \text{Pa} \cdot \text{s}$) [37], r is the radius of the droplet ($3 \times 10^{-3} \text{m}$), and v is the velocity ($0.005 \text{ m} \cdot \text{s}^{-1}$).

will act on the droplet.

On the other hand, the horizontal force act on a spherical shaped rigid body, which is caused by the interfacial tension gradient, can be described as follows [1]:

$$F = \frac{8}{3}\pi r^2 \frac{d\sigma}{dx} \tag{3}$$

where r is the radius, and $\frac{d\sigma}{dx}$ is the interfacial tension gradient.

Therefore, if it is assumed that the droplet is incompressible and rigid, the required $\frac{d\sigma}{dx}$ value to obtain the force corresponds to the above-mentioned viscous friction, $5.74 \times 10^{-5} \text{N}$, is $0.762 \text{ N} \cdot \text{m}^{-2}$ which is relatively small.

The movement of the droplet might also be caused by Marangoni convection in the molten metal droplet due to the interfacial tension gradient caused by the nitrogen concentration gradient along with the contour of the droplet. During the experiment, the nitrogen is dissolving from the bottom of BN crucible, i.e. the nitrogen concentration at the bottom of the droplet is relatively higher than that of the higher

part of the droplet. Therefore, the Marangoni convection will be generated from the bottom part, where the interfacial tension is low (σ_L , σ_R), to the top part of the droplet, where the interfacial tension (σ_T) is higher than σ_L and σ_R , along with the slag-metal interface of the droplet (see Fig. 3). As a consequence of the generation of Marangoni convection, downward convection will be formed at a centre part of the droplet, and circulation will take place until the interfacial tension gradient disappears. In practice, the asymmetric Marangoni flow convections will be formed in the droplet due to the asymmetric distribution of nitrogen, and the droplet will be moved by the asymmetric convections.

It is difficult to estimate the contribution of each driving force mentioned above from the experiment, but the movement of the droplet will be dominated by these two factors. In the following sections, some calculations were performed to estimate the velocity of Marangoni convection.

Velocity of Marangoni convection

In a system where the temperature gradient, concentration gradient, and/or electrical capillarity (electric potential gradient ψ) exists along the x-direction of the interface, the surface/interfacial shear stress τ_s induced by the surface/interfacial tension gradient is expressed as

$$\tau_s = \frac{d\sigma}{dx} = \frac{\partial\sigma}{\partial T} \cdot \frac{dT}{dx} + \frac{\partial\sigma}{\partial c} \cdot \frac{dc}{dx} + \frac{\partial\sigma}{\partial\psi} \cdot \frac{d\psi}{dx} \quad (4)$$

where σ is the surface/interfacial tension, T is the temperature, c is the concentration, and ψ is the electric potential[1].

The liquid flow generated by this shear stress is obtained by solving the equations of motion (Navier–Stokes equations) and thermal conduction equation or diffusion equation under the boundary condition that gives the surface/interfacial tangential force [1].

The Marangoni convection induced by the nitrogen concentration gradients along with the contour of the metal droplet was studied by a coupled transient simulation including two-phase laminar flow and a level-set moving interface. A half-symmetry FE model of the metal droplet was created in the commercially available COMSOL Multiphysics 5.4. Initial droplet shape and dimensions were adopted from the experimental observations. The droplet radius was set as 2 mm, and the contact angle with the

horizontal wetted surface was 100° . The slag/gas initial temperature was set to 1873 K.

In the present experiments, the nitrogen was supplied from the bottom side of the molten iron droplet, and thus in the calculation, the lower surface tension values were given for the lower part of the droplet and higher surface tension values for the higher part of the droplet. It is assumed that the nitrogen distribution and the shape of the droplet are symmetric, and the half part of the droplet was considered in the calculation. An example of the droplet shape is shown in Fig. 4. The blue region is the molten iron, and the red region is the molten slag. The pure white curvature is the contour of the droplet, which corresponds to Gibbs' dividing surface. The shape of the droplet was decided so that it satisfies the Laplace's equation in which the balance between gravity and pressure difference are considered (Eq. 5).

$$\rho g(h - z) + (p^\alpha - p^\beta) = \sigma \left(\frac{1}{r_1} + \frac{1}{r_2} \right) \quad (5)$$

where ρ is the density, g is the gravitational acceleration, h is the height of the droplet, z is the height at a point on the contour of the droplet, p^α is the pressure in the droplet, p^β is the outside pressure, σ is the surface/interfacial tension, and r_1 and r_2 are the two principal radii of curvature of the surface/interface.

Note that the contour in black colour in Fig. 3 is just an initial contour for the calculation which does not satisfy Eq. 5.

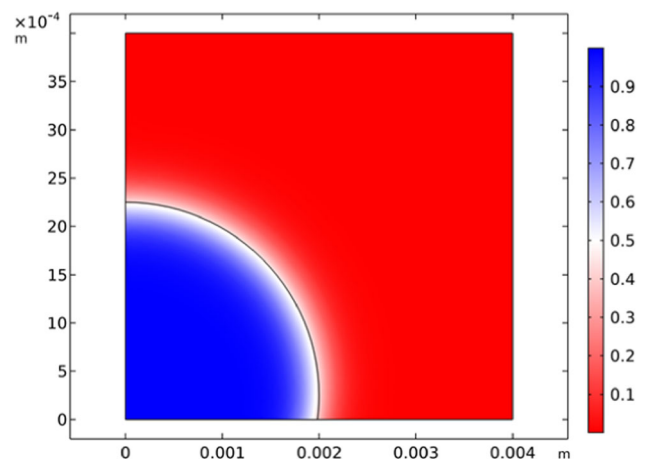


Figure 4 An example of droplet shape in the calculation.

Velocity of Marangoni convection (Gas-Metal system)

To calculate the velocity of Marangoni convection, the surface tension gradient, i.e. the concentration gradient of nitrogen must be known. However, it is next to impossible to know the nitrogen concentration gradient along with the contour of the droplet during the experiment. Therefore, first of all, it was attempted to calculate the velocity of Marangoni convection for the case of gas-metal droplet system to estimate the surface tension gradient by comparing the calculated velocity with the literature values.

In the calculation, the pressures of the molten iron and gas phase are set so that it holds Eq. 5. The contact angle between molten iron droplet and substrate (bottom of the BN crucible) is set as 100°. For the viscosity and density of pure iron droplet, the values at 1873 K, i.e. $5.02 \times 10^{-3} \text{ Pa} \cdot \text{s}$ and $6977 \text{ kg} \cdot \text{m}^{-3}$ were used [38]. The influence of nitrogen on the viscosity and density is negligible, and thus, above values are used for whole calculation. For the gas phase, the properties of argon gas were used. The viscosity of argon gas at 1873 K was estimated as $8.54 \times 10^{-5} \text{ Pa} \cdot \text{s}$ [39]. The density of argon gas at 1873 K was estimated as $0.256 \text{ kg} \cdot \text{m}^{-3}$ by Van der Waals equation with Van der Waals constants $a = 1.355 \text{ bar} \cdot \text{L}^2 \cdot \text{mol}^{-2}$ and $b = 0.0320 \text{ L} \cdot \text{mol}^{-1}$ [40].

According to Keene [32], the surface tension of the Fe–N system can be described by the following equation:

$$\sigma_{\text{Fe-N}} = \sigma_{\text{Fe}} - 1.4 \times (\text{at.}\% \text{N}) \text{N} \cdot \text{m}^{-1} \tag{6}$$

i.e.

$$\sigma_{\text{Fe-N}} = \sigma_{\text{Fe}} - 1.4 \times \frac{100 \times 55.8 \times [\text{mass}\% \text{N}]}{14 \times (100 - [\text{mass}\% \text{N}]) + 55.8 \times [\text{mass}\% \text{N}]} \text{N} \cdot \text{m}^{-1} \tag{7}$$

where σ_{Fe} is the surface tension of pure iron and at 1873 K the surface tension value is $1.877 \text{ N} \cdot \text{m}^{-1}$ [41].

The theoretical treatment of the surface/interfacial tension in the nonequilibrium state as found in the present experiment has not been established, and even the meaning of the surface/interfacial tension in the nonequilibrium state is not clearly defined. Therefore, in the present discussion, it is assumed that the values of surface/interfacial tension are the same as that of equilibrium state for simplicity.

According to a thermodynamic data [42], the solubility of the nitrogen into molten iron at 1873 K is

0.046 mass% under 1 bar nitrogen, and from Eq. 7, the surface tension under this condition is $1.621 \text{ N} \cdot \text{m}^{-1}$. If the top part of the droplet is still pure iron and the bottom part of the droplet is saturated by nitrogen, the surface tension difference between these two locations becomes $0.256 \text{ N} \cdot \text{m}^{-1}$. This is a maximum surface tension difference, but even if it happened, it could be achieved at the only very early stage of the process. Once the diffusion of nitrogen and mass transfer by the Marangoni convection takes place, the surface tension gradient will become less.

The velocity calculations were performed by giving different surface tension difference, $\Delta\sigma$, between the top of the droplet and the bottom part of the droplet. Hirashima et al. [43] measured the surface velocity of the Marangoni convection caused by the nitrogen concentration gradient on the surface of molten iron. In their experiments, the concentration of the nitrogen at the nitrogen gas impinged area was estimated as 0.0425 mass%N, which corresponds to $1.640 \text{ N} \cdot \text{m}^{-1}$ in the surface tension value and the concentration of nitrogen at the point 42 mm away was 0.001 mass%N, which corresponds to $1.871 \text{ N} \cdot \text{m}^{-1}$ in the surface tension value. Therefore, the surface tension gradient can be calculated as $5.5 \text{ N} \cdot \text{m}^{-2}$. In our study, the length of the contour of the droplet from bottom to top is 3.5 mm, and thus the same surface tension gradient, $5.5 \text{ N} \cdot \text{m}^{-2}$ will be achieved when the surface tension difference between bottom and top, $\Delta\sigma$, is $0.02 \text{ N} \cdot \text{m}^{-1}$.

The calculation result when the surface tension difference, $\Delta\sigma = 0.02 \text{ N} \cdot \text{m}^{-1}$, is shown in Fig. 5. As expected, the convection from the lower surface tension region (bottom part of the droplet) to the higher

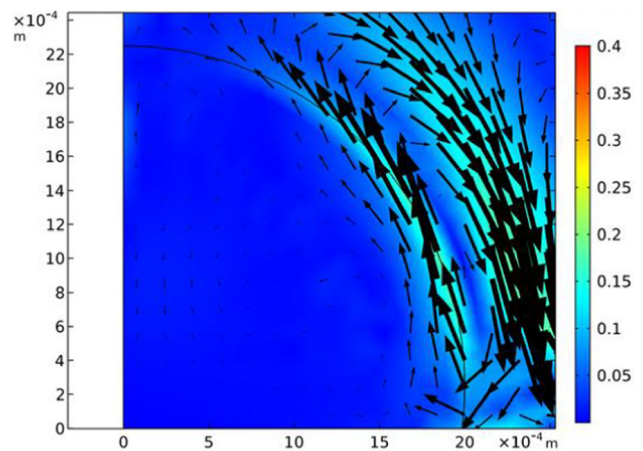


Figure 5 Velocity of Marangoni convection (Metal-Gas system).

surface tension region (top part of the droplet) along with the surface of the droplet, i.e. Marangoni convection was found. In addition, the downward stream from the top of the droplet to the bottom, which is induced by the Marangoni convection was found. As shown in Fig. 5, the calculation result shows that the surface velocity is approximately $0.1\text{--}0.15\text{ m}\cdot\text{s}^{-1}$, and this value agrees with the literature values (experimental values), e.g. $0.08\text{--}0.12\text{ m}\cdot\text{s}^{-1}$ [19] and $0.05\text{--}0.11\text{ m}\cdot\text{s}^{-1}$ [43].

From the above-mentioned calculation result, it was found that the Marangoni convection is induced by even small surface tension difference such as $0.02\text{ N}\cdot\text{m}^{-1}$. In addition, the convection in the gas phase was also found along with the surface of the droplet, although it is microscale. Such convection might influence on the mass transfer in the gas phase and consequently the rate of nitrogen (and other components) removal from molten iron.

Velocity of Marangoni convection (Slag-Metal system)

As the calculation method of the surface velocity is verified with the gas-metal system, it was attempted to apply the method for the slag-metal system. The calculation of the velocity of Marangoni convection for the slag-metal droplet system was done in a similar manner. For the viscosity and density of molten slag, the values at 1873 K , i.e. $203 \times 10^{-3}\text{ Pa}\cdot\text{s}$ [37] and $2783\text{ kg}\cdot\text{m}^{-3}$ [44] were used.

The calculation results are shown in Fig. 6. In addition to the result for $\Delta\sigma = 0.02\text{ N}\cdot\text{m}^{-1}$, the results for $\Delta\sigma = 0.03$ and $0.04\text{ N}\cdot\text{m}^{-1}$ are also shown for the comparison. As can be seen from these figures, even for the slag-metal system, the convection along with the interface, i.e. Marangoni convection and the downward stream at the centre part are generated. However, for the $\Delta\sigma = 0.02\text{ N}\cdot\text{m}^{-1}$ case, the velocity at the molten iron-molten slag interface becomes approximately $0.01\text{--}0.015\text{ m}\cdot\text{s}^{-1}$ which is approximately ten times slower compared to the results for the gas-metal droplet system case. As can be seen in these figures, it is also obvious that the velocity becomes slower with decreasing of interfacial tension gradient.

In the case of the slag-metal system, the denitrification by the slag [45] must be considered. However, in the present case, even if a certain level of denitrification occurs, it will take place uniformly at the

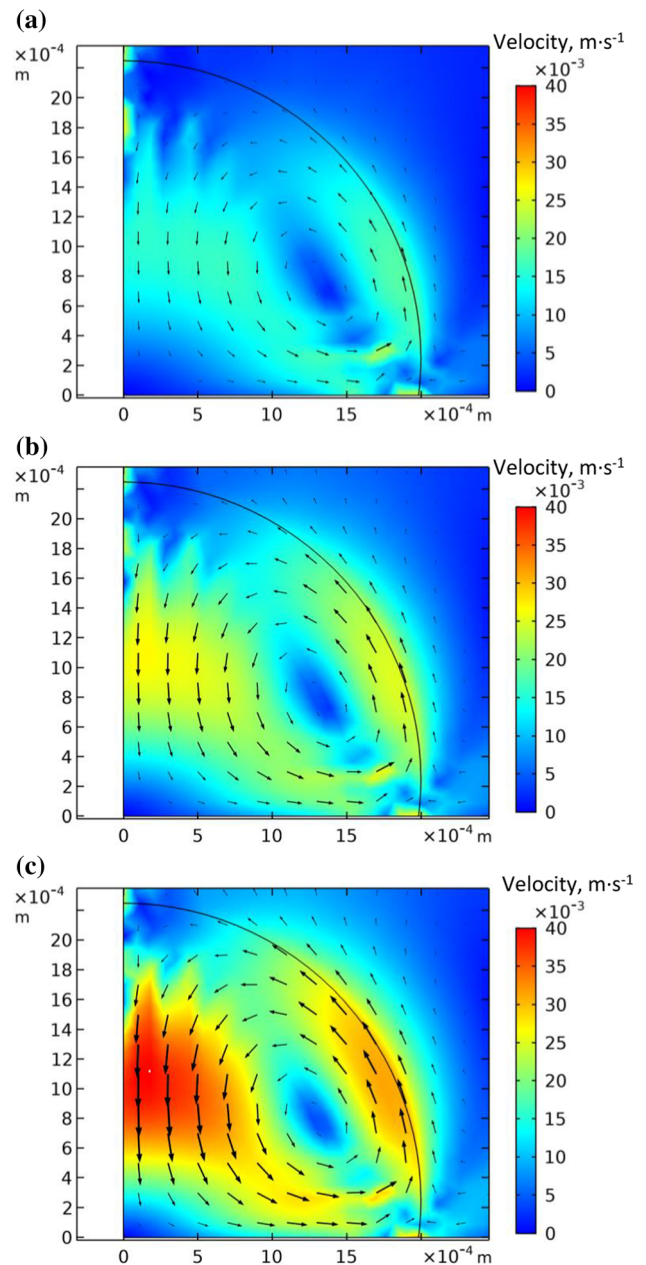


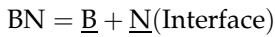
Figure 6 Calculation results (slag-metal system) **a** $\Delta\sigma = 0.02\text{ N}\cdot\text{m}^{-1}$, **b** $\Delta\sigma = 0.03\text{ N}\cdot\text{m}^{-1}$, **c** $\Delta\sigma = 0.04\text{ N}\cdot\text{m}^{-1}$.

slag-metal interface. Hence, the concentration gradient of nitrogen along with the contour of the droplet will be kept constant. As can be seen from Eq. 6, surface tension decreases linearly with increasing of nitrogen, i.e. the gradient is constant in the whole concentration range. Hence, it can be concluded that there is no significant influence of denitrification on the surface tension gradient.

Apparent mass transfer coefficient

In the case of the present system, the absorption of nitrogen into molten iron droplet can be described as follows:

1) Chemical reaction at the solid BN and molten iron interface



2) Transport of nitrogen atoms from the interface to the bulk

$$\underline{\text{N}}(\text{Interface}) = \underline{\text{N}}(\text{Bulk})$$

Iyengar and Pehlke [35] assumed that the reaction 1 is fast enough compared to the diffusion process and made a kinetic model, and the experimental results were reasonably explained. Therefore, it is assumed that the reaction 1 is fast enough in the present study as well.

Regarding the reaction 2, it will occur by both diffusion and convection (Marangoni convection), but Zhu and Mukai [19] concluded that the ‘mass transfer by convection is much more effective’, and they derived an equation for the relation between surface velocity and apparent mass transfer coefficient, K'_m , in the molten iron by the convection as follows. The equation was obtained by fitting the experimental data between approximately $0.017 \leq v \leq 0.098 \text{ m} \cdot \text{s}^{-1}$.

$$K'_m = 0.0684v^{0.7} \tag{8}$$

where v is the surface flow velocity.

According to the surface velocity calculation in the previous section, the surface velocity was approximately $0.02\text{--}0.03 \text{ m} \cdot \text{s}^{-1}$ when the surface tension difference is $0.02\text{--}0.04 \text{ N} \cdot \text{m}^{-1}$. Therefore, the apparent mass transfer coefficient becomes $4.42\text{--}5.88 \times 10^{-3}$ which is relatively small. The smaller K'_m , i.e. the weaker Marangoni convection implies that the reaction 2 is the rate-determining step (it becomes more dominant), in other words, the absorption rate of nitrogen in molten iron from solid BN influenced by the mass transfer in the metal.

Interfacial tension between molten metal and molten slag

The sessile drop method to measure the surface tension or interfacial tension is well-known, but

mechanically and thermodynamically equilibrium state of the droplet is required for the measurements. In the present experiment, the nitrogen is always supplied to the molten metal, and Marangoni convection is induced, and the nitrogen amount and its distribution are changed by time. Therefore, it can be easily imagined that the droplet is not reached at mechanically and thermodynamically equilibrium state. Nevertheless, the interfacial tension was measured using an X-ray photo which was taken the later stage of the observation (after 30 min of observation) by assuming that the droplet reached the equilibrium state. The (apparent) interfacial tension was measured by the Bashforth and Adams' method [46]. The apparent interfacial tension was calculated as $1.93 \text{ N} \cdot \text{m}^{-1}$.

Apart from the measurement, the interfacial tension between molten slag and molten metal, $\sigma_{\text{Metal-Slag}}$, at equilibrium state was estimated using Girifalco-Good's relation [47].

$$\sigma_{\text{Metal-Slag}} = \sigma_{\text{Metal}} + \sigma_{\text{Slag}} - 2\phi(\sigma_{\text{Metal}} \cdot \sigma_{\text{Slag}})^{0.5} \tag{9}$$

where σ_{Metal} is the surface tension of metal, σ_{Slag} is the surface tension of slag, and ϕ is the characteristic of the system.

ϕ for $\text{Al}_2\text{O}_3\text{-CaO-SiO}_2$ system is given by the following equation [48, 49].

$$\phi = 0.0046(\% \text{Al}_2\text{O}_3) + 0.005973(\% \text{SiO}_2) + 0.005806(\% \text{CaO}) \tag{10}$$

where $(\% \text{Al}_2\text{O}_3)$ is the mass% of Al_2O_3 , $(\% \text{SiO}_2)$ is the mass% of SiO_2 , $(\% \text{CaO})$ is the mass% of CaO .

In the case of slag in the present system, $\phi = 0.5395$

The surface tension of the slag, which is required for the calculation by the Girifalco-Good's relation was obtained from literature as $0.59 \text{ N} \cdot \text{m}^{-1}$ at 1873 K [50]. The surface tension of the pure iron at 1873 K is $1.877 \text{ N} \cdot \text{m}^{-1}$ [32].

Hence, the interfacial tension between molten slag and molten iron of the present system at equilibrium state was estimated as follows.

$$\sigma_{\text{Metal-Slag}} = 1.877 + 0.59 - 2 \times 0.5395(1.877 \cdot 0.59)^{0.5} = 1.332 \text{ N} \cdot \text{m}^{-1} \tag{11}$$

It is known that even if the composition of the slag is different, the interfacial tension is similar to a certain extent (about $\pm 0.150 \text{ N} \cdot \text{m}^{-1}$), and the concentration of the surface-active element in the molten

iron is the dominating factor affecting interfacial tension[51]. Therefore, it is assumed that the nitrogen amount dependency on the interfacial tension of Fe–N–Slag system is the same as that of surface tension case (i.e. $1.4 \times (\text{at.\%N})$). From the interfacial tension value of the slag-pure iron by Girifalco-Good's relation ($1.322 \text{ N} \cdot \text{m}^{-1}$) and this nitrogen amount dependency, the interfacial tension value of the Fe–N–Slag system was calculated as $1.293 \text{ N} \cdot \text{m}^{-1}$ (0.007mass\%N).

The apparent interfacial tension which is measured by Bashforth and Adams' method using the X-ray photo taken in the present study ($1.93 \text{ N} \cdot \text{m}^{-1}$) is extremely high compared to the estimated value at equilibrium state by Girifalco-Good's relation ($1.332 \text{ N} \cdot \text{m}^{-1}$) and the results from a parabolic flight experiment ($1.222 \text{ N} \cdot \text{m}^{-1}$ at 1953 K)[52]. It implies that in the present experiment, even after 30 min, the sessile drop is not reached equilibrium state and the convection and/or mechanical imbalance still exist. It corresponds to the fact that the droplet was still moving, although the movement was moderate after 30 min.

Conclusion

The interfacial phenomena between molten iron and molten slag with nitrogen were directly observed using an X-ray radiographic apparatus. In addition, the velocity of the Marangoni convection in the iron drop was calculated using a multiphysics model. The directly observed movement of the sessile drop was attributed to the asymmetric Marangoni convection and force balance caused by the asymmetric distribution of surface-active element (nitrogen). The velocity of the Marangoni convection for the Gas-Metal system was reasonably agreed with the literature values. For the Slag-Metal system case, the velocity becomes approximately ten times slower. The apparent interfacial tension between the molten iron and slag was measured using the X-ray image after 30 min holding. From the apparent interfacial tension value, it was concluded that the system had not reached equilibrium, and the cause of the movement of the sessile drop was attributed to the nonequilibrium state.

Acknowledgements

This research was funded by the Swedish National Space Agency (contract numbers: 120/14 and 117/15), and supported by the Japan Aerospace Exploration Agency (JAXA, the MEXT-Support Program for the Strategic Research Foundation at Private Universities, 2015-2019). We appreciate their support.

Funding

Open Access funding provided by Jönköping University.

Data availability

The data required to derive the conclusion of the present study are given in the manuscript.

Compliance with ethical standards

Conflict of interest The authors declare that there is no conflict of interest.

Open Access This article is licensed under a Creative Commons Attribution 4.0 International License, which permits use, sharing, adaptation, distribution and reproduction in any medium or format, as long as you give appropriate credit to the original author(s) and the source, provide a link to the Creative Commons licence, and indicate if changes were made. The images or other third party material in this article are included in the article's Creative Commons licence, unless indicated otherwise in a credit line to the material. If material is not included in the article's Creative Commons licence and your intended use is not permitted by statutory regulation or exceeds the permitted use, you will need to obtain permission directly from the copyright holder. To view a copy of this licence, visit <http://creativecommons.org/licenses/by/4.0/>.

References

- [1] Mukai K, Matsushita T (2019) Interfacial Physical Chemistry of High-temperature Melts. CRC Press, Florida
- [2] Ed. by Ueno I, Matsumoto S, Watanabe M (2019) Microgravity experiments on Marangoni convection- MEIS,

- Dynamic Surf, and toward JEREMI-. *Int. J. Microgravity Sci. Appl.* 36: 360201–1–360207–7.
- [3] Watanabe M, Tanaka T, Tsukada T, Ishikawa T, Tamaru H, Mizuno A (2015) Numerical Evaluation for Measurement Conditions of Interfacial Tension between Molten Slag and Molten Iron by Oscillating Drop Technique in ISS. *Int J Microgravity Sci Appl* 32:320103–1–320103–7
- [4] Nakamura T, Yokoyama K, Noguchi F, Mukai K (1991) Direct Observations of Marangoni Convection in Molten Salts. *Molten Salt Chemistry and Technology, Materials Science Forum, Trans. Tech Publ Switzerland* 73–75:153–158
- [5] Mukai K (1998) Marangoni flows and corrosion of refractory walls. *Phil Trans R Soc Lond A* 356:1015–1026
- [6] Mukai K, Toguri JM, Kodama I, Yoshitomi J (1986) Effect of Applied Potential on the Interfacial Tension between Liquid Lead and PbO–SiO₂ Slags. *Can Metall Q* 25:225–231
- [7] Mukai K, Matsushita T, Seetharaman S (2005) Motion of fine particles in liquid caused by interfacial tension gradient in relation to metals separation technologies. *Scand J Metall* 34:137–142
- [8] Kaptay G (2012) Interfacial forces in dispersion science and technology. *J Dispers Sci Technol* 33:130–140
- [9] Kaptay G (2005) Classification and general derivation of interfacial forces, acting on phases, situated in the bulk, or at the interface of other phases. *J Mater Sci* 40:2125–2131
- [10] Mukai K, Zeze M (2003) Motion of Fine Particles under Interfacial Tension Gradient in Relation to Continuous Casting Process. *Steel Res* 74:131–138
- [11] Mukai K, ed. by Seetharaman S (2005) *Fundamentals of Metallurgy*. Woodhead Publishing Limited, Cambridge, p.246–263.
- [12] Mills KC, Hondros ED, Li Z (2005) Interfacial phenomena in high temperature processes. *J Mater Sci* 40:2403–2409
- [13] Sándor T, Mekler C, Dobránszky J, Kaptay G (2012) An Improved Theoretical Model for A-TIG Welding Based on Surface Phase Transition and Reversed Marangoni Flow. *Metal Mater Trans A* 44:351–361
- [14] Mills KC, Keene BJ, Brooks RF, Shirali A (1998) Marangoni effects in welding. *Phil Trans R Soc Lond A* 356:911–925
- [15] Yin H, Emi T (2003) Marangoni flow at the gas/melt interface of steel. *Metal Mater Trans B* 34:483–493
- [16] Eyer A, Leiste H, Nitsche R. (1984) Crystal Growth Of Silicon On Spacelab 1, Experiment ES-321. In *ESA European Symposium on Material Science Under Microgravity, Results of Spacelab 1, Schloss Elmau, November 5–7, 1984, ESA SP-222*, p. 173–182.
- [17] Byrne M, Belton GR (1983) Studies of the interfacial kinetics of the reaction of nitrogen with liquid iron by the ¹⁵N-¹⁴N isotope exchange reaction. *Metall Trans B* 14:441–449
- [18] Lee J, Morita K (2003) Interfacial Kinetics of Nitrogen with Molten Iron Containing Sulfur. *ISIJ Int* 43:14–19
- [19] Zhu J, Mukai K (1998) The Influence of Oxygen on the Rate of Nitrogen Absorption into Molten Iron and Marangoni Convection. *ISIJ Int* 38:220–228
- [20] Zhu J, Mukai K (1999) The Rate of Nitrogen Desorption from Liquid Iron by Blowing Argon Gas under the Condition of Non-inductive Stirring. *ISIJ Int* 39:219–228
- [21] Mukai K, ed. by Seetharaman S (2005) *Fundamentals of Metallurgy*, Woodhead Publishing Limited, Cambridge, p.246.
- [22] Seetharaman S, Mukai K, Sichen D (2004) Viscosities of slags-an overview. *7th International Conference Molten Slags Fluxes and Salts, Cape Town, The South African Institute of Mining and Metallurgy* 31–41.
- [23] Hahn P-S, Slattery JC (1985) Effect of surface viscosities on the stability of a draining plane parallel liquid film as a small bubble approaches a liquid-gas interface. *AIChE J* 31:950–956
- [24] Edwards DA, Wasan DT (1990) Foam Dilatational Rheology, I. Dilatational viscosity. *J Colloid Interf Sci* 139:479–487
- [25] Agrawal SK, Wasan DT (1979) The effect of interfacial viscosities on the motion of drops and bubbles. *Chem Eng J* 18:215–223
- [26] Edwards EA, Brenner H, Wasan DT (1989) On a relation between foam and surface dilatational viscosities. *J Colloid Interf Sci* 130:266–270
- [27] Matsushita T, Watanabe T, Mukai K, Seetharaman S (2009) Interfacial phenomena between molten steel and slag. *Proceedings of the VIII International Conference on Molten Slags, Fluxes and Salts, 18–21 January 2009, Santiago, Chile, 703–714.*
- [28] Matsushita T, Watanabe T (2011) Dynamic in situ X-ray observation of a molten steel drop shape change in molten slag. *Mineral Processing and Extractive Metallurgy (Trans. Inst. Min Metall. C)*. 120: 49–55.
- [29] Elfsberg J, Matsushita T (2011) Measurements and Calculation of Interfacial Tension between Commercial Steels and Mould Flux Slags. *steel research int.* 82: 404–414.
- [30] Muhmood L, Viswanathan NN, Seetharaman S (2011) Some Investigations into the Dynamic Mass Transfer at the Slag-Metal Interface Using Sulfur: Concept of Interfacial Velocity. *Metall Mater Trans B* 42B:460–470
- [31] Cao W, Muhmood L, Seetharaman S (2012) Sulfur transfer at slag/metal interface–impact of oxygen potential. *Metall Mater Trans B* 43B:363–369

- [32] Keene BJ (1988) Review of data for the surface tension of iron and its binary alloys. *Int Mater Rev* 33:1–37
- [33] Zhu J, Mukai K (1998) The Surface Tension of Liquid Iron Containing Nitrogen and Oxygen. *ISIJ Int* 38:1039–1044
- [34] Ed. by Hino M, Ito K (2010) *Thermodynamic data for steelmaking*. Tohoku University Press, Sendai, p.254.
- [35] Iyengar GNK, Pehlke RD (1970) Dissolution of boron nitride in liquid iron. *Metal Trans* 1:2235–2242
- [36] Ogino K. (1988) *Handbook of physico-chemical properties at high temperatures*, eds. Kawai Y, Shiraishi Y., ISIJ, Japan, 170.
- [37] Siafakas D, Matsushita T, Hakamada S, Onodera K, Kargl F, Jarfors AEW, Watanabe M (2018) Measurement of Viscosity of $\text{SiO}_2\text{-CaO-Al}_2\text{O}_3$ Slag in Wide Temperature Range by Aerodynamic Levitation and Rotating Bob Methods and Sources of Systematic Error. *Int J Microgravity Sci Appl* 35:350204–1-350204–8
- [38] Mills KC (2002) Recommended values of thermophysical properties for selected commercial alloys. Woodhead Publishing Limited, Cambridge
- [39] Macrossan MN, Lilley CR (2003) Viscosity of argon at temperatures >2000 K from measured shock thickness. *Phys Fluids* 15:3452–3457
- [40] Reid RC, Prausnitz JM, Poling BE (1987) *The properties of gases and liquids*, 4th edn. McGraw Hill, New York
- [41] Keene BJ (1993) Review of data for the surface tension of pure metals. *Int Mater Rev* 38:157–192
- [42] Ed. by Hino M, Ito K (2010) *Thermodynamic data for steelmaking*. Tohoku University Press, Sendai, p.247.
- [43] Hirashima N, Choo RTC, Toguri JM, Mukai K (1995) The effect of surface movements on nitrogen mass transfer in liquid iron. *Metall Trans B* 26B:971–980
- [44] Xin J, Gan L, Jiao L, Lai C (2017) Accurate Density Calculation for Molten Slags in $\text{SiO}_2\text{-Al}_2\text{O}_3\text{-CaO-MgO}$ Systems. *ISIJ Int* 57:1340–1349
- [45] Ito K, Fruehan RJ (1988) Thermodynamics of nitrogen in $\text{CaO-SiO}_2\text{-Al}_2\text{O}_3$ slags and its reaction with Fe-C_{sat} melts. *Metall Trans B* 19:419–425
- [46] Bashforth F, Adams JC (1883) An attempt to test the theories of capillary action by comparing the theoretical and measured forms of drops of fluid. Cambridge University Press, Cambridge
- [47] Girifalco LA, Good RJ (1957) A Theory for the Estimation of Surface and Interfacial Energies. I. Derivation and Application to Interfacial Tension. *J Phys Chem* 61:904–909
- [48] Cramb AW, Jimbo I (1989) Interfacial considerations in continuous casting, *Iron and steelmaker*, June: 43–55.
- [49] Cramb AW, Jimbo I (1989) Calculation of the interfacial properties of liquid steel–slag systems. *Steel Res* 60:157–165
- [50] Allibert M, Gaye H, Geiseler J, Janke D, Keene BJ, Kirner D, Kowalski M, Lehmann J, Mills KC, Neuschütz D, Parra R (1995) *Slag Atlas*, 2nd ed., ed. by Verein Deutscher Eisenhüttenleute (VDEh), Verlag Stahleisen, Düsseldorf, 431.
- [51] Ogino K (1988) *Handbook of Physico-chemical Properties at High Temperatures*, ISIJ, ed. Kawai Y and Shiraishi Y, Tokyo, 170.
- [52] Watanabe M (2018) *Measurement of Interfacial Tension and Thermophysical Properties of Molten Steel and Oxides*, Twenties symposium on thermophysical properties, Boulder, CO, USA, June 24–29.

Publisher's Note Springer Nature remains neutral with regard to jurisdictional claims in published maps and institutional affiliations.